Accepted Manuscript

Plasmonic nanoholes as SERS devices for biosensing applications: An easy route for nanostructures fabrication on glass substrates

Patrizio Candeloro, Ernesto Iuele, Gerardo Perozziello, Maria Laura Coluccio, Francesco Gentile, Natalia Malara, Vincenzo Mollace, Enzo Di Fabrizio

Please cite this article as: Patrizio Candeloro, Ernesto Iuele, Gerardo Perozziello, Maria Laura Coluccio, Francesco Gentile, Natalia Malara, Vincenzo Mollace, Enzo Di Fabrizio, Plasmonic nanoholes as SERS devices for biosensing applications: An easy route for nanostructures fabrication on glass substrates, (2016), doi:10.1016/j.mee.2016.12.015

Plasmonic Nanoholes as SERS devices for biosensing applications: an easy route for nanostructures fabrication on glass substrates

Patrizio Candeloro[a*], Ernesto Iuele[a], Gerardo Perozziello[a], Maria Laura Coluccio[a], Francesco Gentile[a,b], Natalia Malara[a,c], Vincenzo Mollace[c], Enzo Di Fabrizio[a,d]

[a] BioNEM Lab., Department of Experimental and Clinical Medicine, Univ. "Magna Graecia" of Catanzaro, 88100 Loc. Germaneto – Catanzaro, Italy

[b] Electrical Engineering and Information Technology Department, University "Federico II" of Naples, 80125 Naples, Italy

[c] Department of Health Sciences, Univ. "Magna Graecia" of Catanzaro, 88100 Loc. Germaneto – Catanzaro, Italy

[d] SMILEs Lab., Physical Science and Engineering Division, KAUST, 23955-6900 Thuwal, Kingdom of Saudi Arabia

*Corresponding author, e-mail: patrizio.candeloro@unicz.it

Abstract

Surface enhanced Raman spectroscopy (SERS) has been largely exploited in the last decade for biochemical and biomedical research. But some issues still require attention before transferring SERS to bioclinical routinely practices, such as reproducibility, quantitative analysis, signal background interference. In this work we propose an easy and cheap route, based on a template stripping technique, for producing plasmonic nanostructured films with SERS capabilities. We focus our attention to nanoholes in a continuous gold film, conversely to the majority of the literature which is dealing with individual nanostructures. Plasmon resonances occur at the holes edges, thus enabling the possibility of SERS signals from biomolecules and the potential application as biosensors. One advantage of the nanoholes patterned film is the optical-subdiffraction pitch, which prevents any Raman and/or fluorescence signal arising from the bottom slide. This effect paves the way to standard glass slides, much cheaper than CaF_2 ones, as suitable substrates for SERS devices, without any interfering signal coming from the glass itself.

Keywords: nanoholes; template stripping; plasmonic nanostructures; SERS spectroscopy

1. Introduction

Surface enhanced Raman spectroscopy (SERS) has attracted large interest in the last decade [1, 2, 3] because of its potentiality to bring sensitivity of biochemical analysis to a single-molecule-detection level [4]. Nowadays it is well-known that SERS effect arise from plasmonic resonances in suitable metal nanostructures, typically in gold and silver ones. Even if SERS is attainable also in disordered and randomly distributed nanoparticles, the Raman signal enhancement strongly depends on size and shape of the particles themselves. Consequently, it has a crucial importance the fabrication of SERS substrates made of well defined and uniform nanostructures, in order to make the SERS approach a powerful quantitative technique. In this framework, different plasmonic elements have been presented in literature [5, 6, 7, 8], and more recently also nanoholes have been reported as suitable devices for plasmonic resonances. So far nanoholes have been used in transmission mode [9], exploiting extraordinary optical transmission (EOT) and EOT coupling to surface plasmons [10]. In the present work instead, we use nanoholes arrays for producing fruitful enhanced Raman signal in backscattering configuration independently from EOT, as earlier reported [11, 12], and the results suggest that the subdiffraction periodicity of nanoholes helps to prevent Raman signal from the device substrate.

We have used a template-stripping technique [13] to produce the plasmonic nanoholes. After fabricating a time consuming and expensive Si template by electron beam lithography (EBL), the pattern can be replicated several times on different optical substrates, also using different metals (Au and Ag for plasmonic purposes). The pattern replication is a straightforward and cheap step, that can be easily afforded also by laboratories not equipped for nanofabrication. Subsequently a well known biomolecule, Rhodamine-6G, at low concentrations has

been used for testing the SERS capabilities of the produced devices. The comparison of Raman measurements performed inside and outside the patterned areas highlights SERS efficiency of the nanoholes, thus confirming their potential application for biosensing devices.

2. Materials and Methods

As already reported by H. Im et al. [13], a Silicon template is produced by a combination of standard high resolution lithography (such as electron beam lithography) and reactive ion etching (RIE) technique. Then the Si template is covered with a thin metal layer, Au in the present work for plasmonic purposes. An usual optical glue is deposited on a glass slide, or different optical component, which will host the pattern duplicate. Subsequently, the glass slide is pressed face down over the Si template, and the glue moves the whole Au thin film with nanostructures from the template to the glass (Fig. 1).

2.1 Silicon template fabrication

The Si template has been fabricated by electron beam lithography and RIE process. Three different patterns of nanoholes have been designed, keeping a fixed pitch of 400nm and changing instead the diameter/spacing duty-cycle of the holes, with diameters of 100, 200 and 300nm. A 200nm layer of PMMA-950K electron resist is deposited over a Si substrate by spinning, followed by a
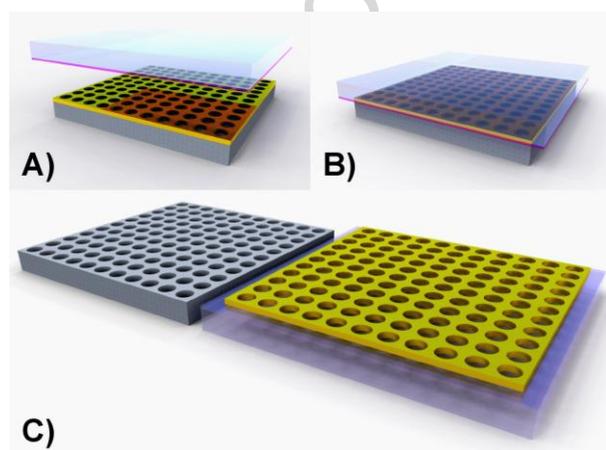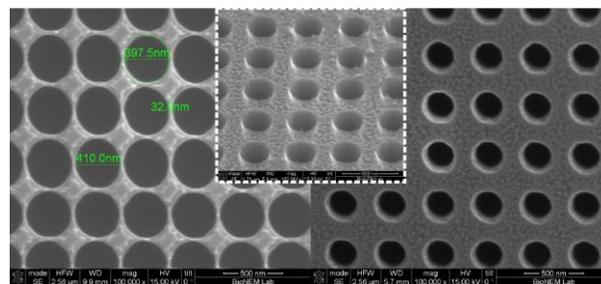
Figure 2. SEM pictures of Si templates fabricated by EBL and ICP-RIE processes. Nanoholes patterns with same spatial pitch but different diameter/spacing duty cycles are produced. The inset shows a tilted view of the pattern.

pre-bake step at 170°C for 5min in order to evaporate the anisole solvent. The patterns are exposed with a dose of $800\mu C/cm^2$ using a 30keV electron beam. The pattern development is carried out in a solution of MIBK:IPA=1:3 at room temperature for 80sec.

Subsequently the resist pattern is used to mask the Si substrate during the RIE process. A inductively-coupled-plasma (ICP-RIE) is used for the dry-etching. The plasma mixture is composed by $C_4F_8/SF_6/Ar$ (60/25/10sccm), the radiofrequency powers for the coil and the platen are imposed to 400 and 15W, respectively, while the pressure during the process is 8.0mTorr. The ICP-RIE process duration is just 150sec, leading to a Si pattern with a thickness of 600nm. Indeed, the aspect ratio of the structures is not a critical parameter for the template stripping, and in the case of a 200nm diameter nanohole a thickness of half micron is enough. Figure 2 shows some results of the Si template fabrication.

2.2 Template stripping and pattern replication

A 50nm thin Au layer is deposited over the Si template, by a thermal physical-vapor-deposition, without any adhesion layer. Obviously the metal film is much thinner than the depth of the holes, and consequently the film on top of the Si template replicates the nanoholes pattern (see Fig. 1A). Then the glass slide is prepared: a drop of UV-activated optical glue (in our case, NOA63 from Norland) is deposited over the transparent glass substrate and slightly smeared on it, in order to reduce the curvature of the drop surface and to move towards a "flat" layer. Then the Si template with the metal film is firmly pressed on it, with the gold layer facing up to the glue (Fig. 1B). For achieving better results in this replication step, the liquid drop of glue could be replaced by a thin film of gluing material, already shaped in the

Figure 1. Schematic view of the process. A): Si-template with Au nanostructured thin film (bottom) and glass-slide with optical glue, face down (top); B): glass slide with glue is pressed over Si template with Au film; C): Au nanostructured film is transferred from Si template (on the left) to the glass slide (on the right).

form of a flat sheet. Through the transparent substrate the glue is activated by means of UV irradiation, thus strongly adhering to the Au nanostructured film. At the end, the glass substrate is removed from the template and, due to the lack of adhesion layer between Si and Au, the nanostructures are completely transferred to the transparent, optical slide (Fig. 1C). The same Si template can be reused several times in this way, after depositing another metal layer. In the case of gold, the metal film has a poor adhesion with the Si template, and before reusing the template an acetone rinsing is enough to remove eventual residuals. However, also other metals with a better adhesion on Si can be used, because the Si substrate can undergo treatments with more aggressive solvents and/or acids for removing fastened metal residuals.

2.3 Raman/SERS analysis

SERS capabilities of nanoholes-on-glass devices are probed by using a well-known biomolecule, Rhodamine-6G, at a concentration of 10^{-6}M in aqueous solution. A 5.0µl drop of solution is deposited over the whole patterned area, covering also the surrounding non-patterned regions. Raman measurements are performed with an Alpha300-RA instrument from Witec GmbH, using a 633nm wavelength laser source in backscattering configuration, and an integration time of 0.15s. The focusing optics is a 100×/0.9NA objective, and the laser power at the sample level is imposed to the small value of 0.1mW/cm^2 for SERS measurements inside the patterned region, while it is increased to the larger value of 5.0mW/cm^2 outside the nanoholes area. All analysis of SERS spectra is carried out by means of a home developed code, Raman Tool Set, freely available [14, 15].

### 3. Results and discussion

Some results of the template stripping process are shown in Fig. 3 for different pattern geometries. Before discussing the SERS measurements, we want to comment some advantages of both the template stripping technique and the nanoholes SERS pattern. The template stripping allows to reproduce in a easy and fast way high resolution patterns on every optical substrate. The fact that glass slides as well as other optical materials (e.g. CaF$_2$ and quartz) can be used is not a minor improvement. Indeed, up to date EBL processes on
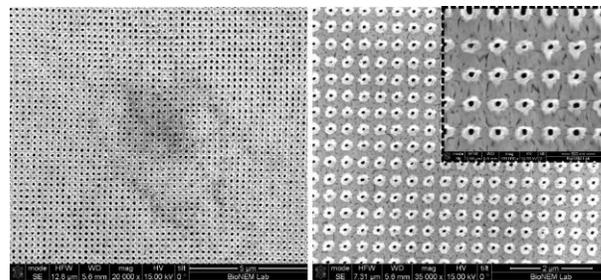
Figure 3. SEM pictures of Au nanoholes patterns sticking on glass slides, after template stripping replication. On the left, an overview of the pattern with 300nm diameter holes; on the right, the pattern with 100nm diameter holes, along with a more detailed view reported in the inset. Some distortions in SEM pictures are due to the local charging of the thick insulating substrate.

insulating materials, as glasses and other optics, are very demanding and tricks are required to avoid local charges and loss of spatial resolution. Instead this approach is in agreement with the idea of other replication techniques, such as nano-imprint lithography, but additionally it avoids the need of any kind of equipment and/or instrument, i.e. even no press machine is needed for transferring the pattern from Si template to optical glue. Once the Si template is produced, any standard optical laboratory equipped with suitable glues, and UV-lamps for activating the glue, can easily reproduce the pattern on several samples, without any nanotechnological instrument.

The other remarkable effect is due to the pattern, and it is the diffraction-limited noise from the background. Raman spectroscopy community well knows the annoying signals coming from standard glasses used in optical microscopy, and the need of more expensive materials as substrates. As examples consider that both an outstanding pioneering work about SERS [16] as well as several following, important applications [17, 18, 19] are dealing with background subtraction. It is worthy to notice that only in the case of Resonant Raman combined with SERS effect, the so-called surface enhanced Resonant Raman scattering (SERRS), the characteristic peaks of the molecule undergoing Resonant Raman are so largely amplified that further background subtraction is not required. Instead in the present case the pitch of the pattern is beyond the optical diffraction limit, and this actually stops the Raman signal arising from both glue and glass below the Au nanoholes. Consequently we do not observe any background signal in backscattering configuration during SERS measurements, and this is not due to the small laser power. In fact the same small laser
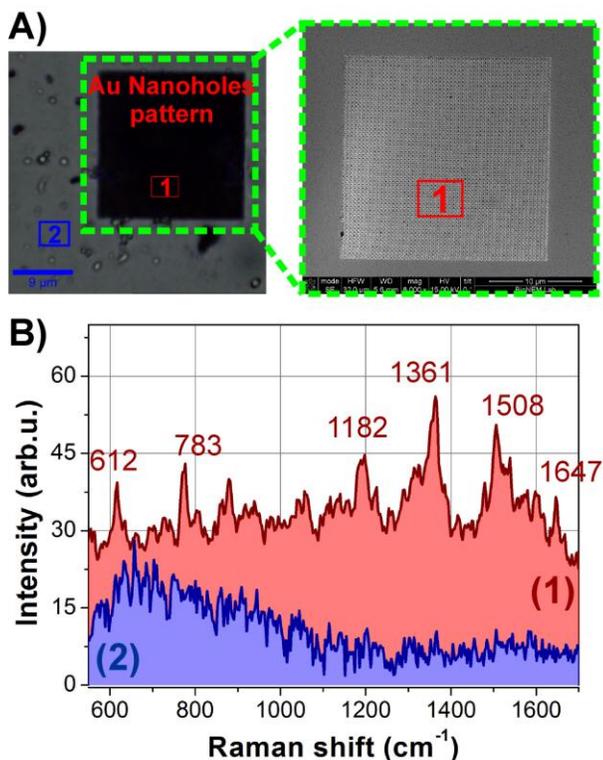
Figure 4. Rhodamine-6G in aqueous solution with a concentration of 10^{-6}M is deposited over the pattern and the surrounding regions. A) Raman measurements are performed both inside (1) and outside (2) the nanoholes pattern: a small laser power of 0.1mW/cm^2, typical for SERS probing, is used inside; instead outside the pattern the power is increased up to 5.0mW/cm^2. B) typical Raman spectra recorded on the sample: the red curve (1) measured inside the pattern exhibits clear peaks of Rhodamine-6G while the blue curve (2) from outside does not show any clear peak. Remarkably, both the curves do not exhibit any Raman signature from the glue and/or glass below the Au pattern.

power allows to detect, through SERS, the few biomolecules in intimate contact with nanostructures on the top of the Au pattern. But at the bottom side we have a large amount of glue in intimate contact with the pattern as well, and no signal from the glue is observed. Indeed, only if EOT conditions were fulfilled by the incident light it would be possible to transmit light beyond the nanoholes array, and to excite Raman signals from the glue/glass system.

Coming to SERS probing, we have used the well-known benchmark Rhodamine-6G [20, 21, 22] as testing biomolecule, with a 10^{-6}M concentration in aqueous solution. A drop of solution is deposited over the array of nanoholes with 200nm diameter, covering both the patterned film and the surrounding regions. Subsequently SERS measurements are performed in different areas inside and outside the pattern (Fig. 4A). We have used a

633nm laser source, which is the most suitable laser line for exciting surface plasmons in our nanostructures. S.-H. Chang *et al*. [23] have simulated the electric field distribution over an array of Au nanoholes on glass and immersed in air, with geometric parameters (nanoholes with a 200nm diameter and a 100nm thick Au film) similar to our nanostructures. They have found that plasmon resonances occur when the incident light has a wavelength of about 630nm, and that a high enhancement of the local electric field on the top of the nanostructures is then observed. Instead only wavelengths larger than 650nm are producing significant electric fields at the bottom side of the nanostructured Au film, where the glue layer is present. This means that the incident 633nm laser light is stimulating SERS signals from the top layer through the excitation of LSPR modes (localized surface plasmon resonance) [12], without any EOT transmission through the nanoholes array (which instead would require the excitation of surface plasmon polariton modes, SPP).

In our measurements, typical characteristic peaks from Rhodamine-6G are observed only from the patterned area (Fig. 4B), while outside no significant peak is detected despite the increased laser power (from 0.1 up to 5.0mW/cm^2). More in details the average spectrum from patterned region clearly exhibits Raman signatures at 612cm^{-1} due to out-of-plane (op) xanthenes-ring-deformation (XRD), at 783cm^{-1} for the in-plane (ip) XRD, 1182cm^{-1} assigned to a combination of ip-XRD with bending of C–H and N–H bonds, at 1361cm^{-1} for xanthenes-ring-stretching (XRS) and ip C–H bending, at 1508cm^{-1} due to XRS, C–N stretching and C–H bending, and finally at 1647cm^{-1} because of XRS and ip C–H bending (for peaks assignments see for example ref. [20]). As mentioned above, no signal from the glue is observed: *i*) outside the pattern we have a 50nm thick continuous Au-film which masks completely the underlying glue; *ii*) inside the pattern we have holes, but the subdiffraction pitch of the nanostructures prevents any optical access to and from the bottom side.

Finally, we want to highlight that peaks intensities observed in Fig. 4B well compare with other former works. Even if a straight comparison is difficult because of the many parameters involved in SERS experiments (such as the metal material, periodicity and shapes of nanostructures, wavelength and power of the laser source, concentration of the testing molecule), we can at least normalize peak intensities by laser power, R6G concentration and integration time. In this way we can

compare our SERS results with other works dealing with Au nanoholes. J.T. Bahns et al. [24] report SERS spectra of $70 \cdot 10^{-6}$M R6G on a hexagonal nanoholes Au pattern with 200nm periodicity and 140nm diameter holes, and the maximum peak intensity is $30 \cdot 10^3$ counts with an integration time of 80s and a 633nm laser power of 1.0mW. Normalizing this result to 10^{-6}M R6G (like it is in the present work) and dividing by the integration time, a maximum peak intensity of 6CPS (counts-per-second) is obtained. Considering that in the present work the integration time is just 0.15s, the R6G spectrum of Fig. 4B leads to about 165CPS, thus achieving a much better result (without taking into consideration that the laser power is just 0.1mW in the present work). D. Choi et al. [25] measure SERS spectra of R6G 10^{-6}M over a hexagonal nanoholes Au pattern with periodicity of 100nm, hole diameter of 30nm and below, different Au thickness from 10 up to 100nm. With a laser power of 90mW and an integration time of 10s, the maximum peak intensity reported in ref. [25] is 300counts, leading to 30CPS when only the integration time is taken into account (again without normalizing to the laser power). Also in this comparison, the SERS intensities (measured as CPS) achieved in our work are remarkable. If we also consider the work of W. Yue et al. [26], where SERS spectra of R6G $5 \cdot 10^{-5}$M are measured over several kinds of gold nanostructures with periodicity from 160 up to 320nm, we find therein a maximum peak intensity of 2500CPS with a 533nm laser source (power is not reported in that work). Despite the 533nm wavelength which produces resonant SERS, the normalization of that intensity by the R6G concentration leads to 50CPS, which is still below our result of 165CPS.
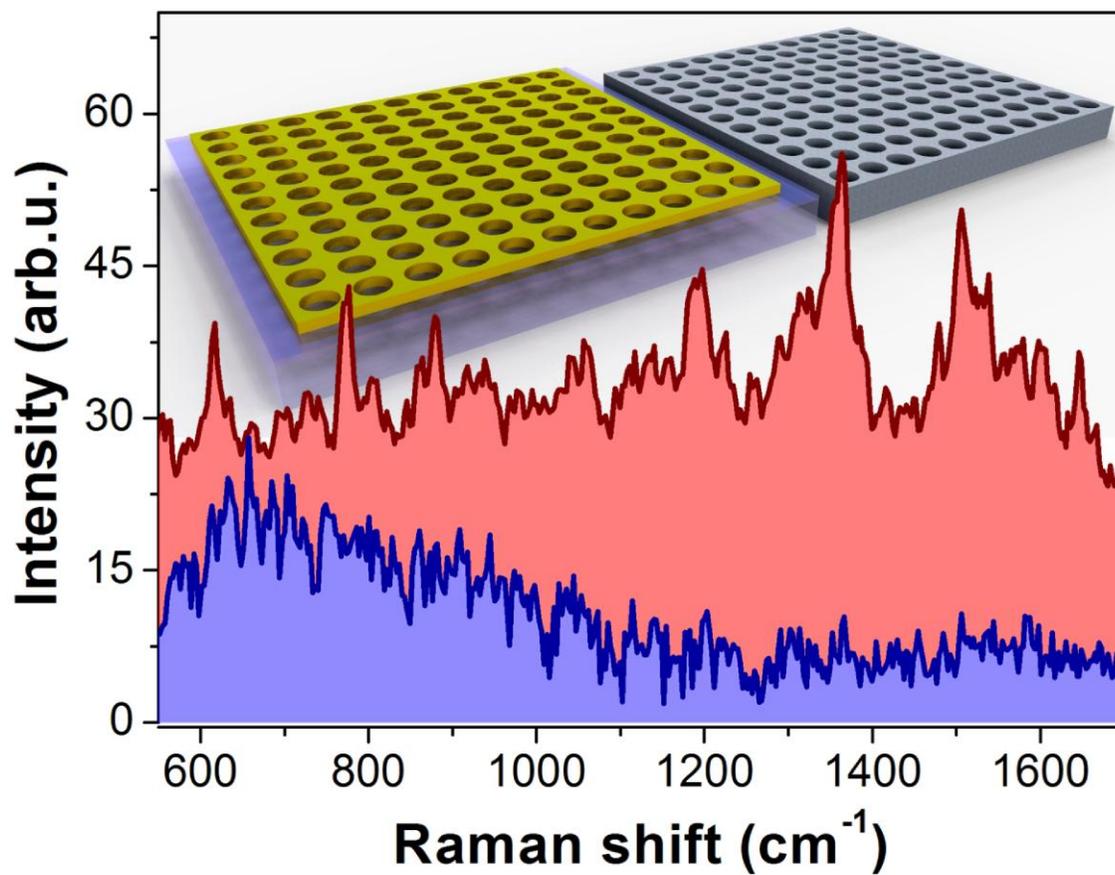
4. Conclusions

In the present work we have exploited a template stripping approach for fabricating patterns of Au nanoholes on insulating, optical materials. The template stripping resulted to be a suitable technique for easy and fast reproduction of patterns with high spatial resolution, and it offers significant advantages for a future mass production of SERS substrates constituted by ordered and uniform nanostructures. Indeed it is a very low cost protocol and no high technological, expensive instruments are required. Up to date some deformations are still present in the replica of the patterns, but the overall geometry with the spatial resolution is preserved. Further improvements could be achieved with a more defined glue layer, such as a thin, dense sheet of gluing material with nearly flat surfaces. The Au patterns, duplicated on optical-microscopy glass slides, successfully worked as SERS substrates, allowing the detection of small Rhodamine-6G concentrations with small laser power. More remarkably, no Raman signal is detected from the bottom side of the Au pattern, neither from the glue nor from the glass, thanks to the subdiffraction pitch of the nanoholes. This latter result has a major importance for the Raman spectroscopy community.

Acknowledgements

References

[1] P.L. Stiles, J.A. Dieringer, N.C. Shah, R.P. Van Duyne, Annual Review of Analytical Chemistry **1**, 601-626 (2008)

[2] M.L. Coluccio, F. Gentile, G. Das, A. Nicastri, A.M. Perri, P. Candeloro et al., Science Advances **1(8)**, e1500487 (2015)

[3] F. Gentile, G. Das, M.L. Coluccio, F. Mecarini, A. Accardo et al., Microelectronic Engineering **87(5–8)**, 798–801 (2010)

[4] K. Kneipp, Y. Wang, H. Kneipp, et al., Phys. Rev. Lett. **78** (1997) 1667-1670

[5]   F. De Angelis, F. Gentile, F. Mecarini, G. Das, et al., Nature Photonics **5** (2011), 682-687

[6]   M.J. Banholzer, J.E. Millstone, L. Qin, C.A. Mirkin, Chem. Soc. Rev. **37**, 885-897 (2008)

[7]   J.F. Li, Y.F. Huang, Y. Ding, Z.L. Yang, S.B. Li, X.S. Zhou, F.R. Fan, W. Zhang et al., Nature 464, 392-395 (2010)

[8]   F. Gentile, M.L. Coluccio, N. Coppedè, F. Mecarini, G. Das et al., ACS Appl. Mater. Interfaces **4(6)**, 3213–3224 (2012)

[9]   A.G. Brolo, E. Arctander, R. Gordon, B. Leathem, K.L. Kavanagh, Nano Lett. **4** (2004), 2015-2018

[10]   T.W. Ebbesen, H.J. Lezec, et al., Nature **391** (1998), 667-669

[11]   Q. Yu, P. Guan, D. Qin, G. Golden, P.M. Wallace, Nano Lett., **8** (2008), 1923-1928

[12]   P. Zheng, S.K. Cushing, S. Suri, N. Wu, Physi. Chem. Chem. Phys., **17** (2015), 21211-21219

[13]   H. Im, S.H. Lee, N.J. Wittenberg, et al., ACS Nano **5(8)** (2011), 6244-6253

[14]   P. Candeloro, E. Grande, R. Raimondo, D. Di Mascolo, F. Gentile, M.L. Coluccio, G. Perozziello, N. Malara, M. Francardi, E. Di Fabrizio, Analyst **138** (2013), 7331.

[15]   Raman Tool Set is available for free at the address: http://ramantoolset.sourceforge.net

[16]   S. Nie, S.R. Emory, Science **275** (1997), 1102.

[17]   X. Zhang, N.C. Shah, R.P. van Duyne, Vibrational Spectroscopy **42** (2006), 2-8

[18]   M. Fan, G.F.S. Andrade, A.G. Brolo, Analytica Chimica Acta **693** (2011), 7-25

[19]   P. Roesch, M. Schmitt, W. Kiefer, J. Popp, Journal of Molecular Structure **661-662** (2003), 363-369

[20]   L. Jensen, G.C. Schatz, Journal of Physical Chemistry A **110** (2006), 5973-5977

[21]   J. Chowdhury, P. Pal, M. Ghosh, T.N. Misra, Journal of Colloid and Interface Science **235** (2001), 317–324

[22]   Y.-C. Liu, C.-C. Yu, S.-F. Sheu, Journal of Materials Chemistry **16** (2006), 3546-3551

[23]   S.-H. Chang et al., Optics Express, 2005, **13(8)**, 3150.

[24]   J.T. Bahns, Q. Guo, J.M. Montgomery, S.K. Gray, H.M. Jaeger, L. Chen, J. Phys. Chem. C Nanomater. Interfaces **113(26)** (2009), 11190-11197

[25]   D. Choi, Y. Choi, S. Hong, T. Kang, L.P. Lee, Small **6(16)** (2010), 1741-1744

[26]   W. Yue, Z. Wang, Y. Yang, L. Chen, A. Syed, K. Wong, X. Wang, J. Micromech. Microeng. **22** (2012), 125007

Graphical abstract